AGU ADVANCING EARTH AND SPACE SCIENCE

Geophysical Research Letters®

RESEARCH LETTER
10.1029/2021GL096135

Key Points:

- We examine the diversity of ST anomalies related to weak, moderate and strong El Niño and Southern Oscillation (ENSO) events in North America forced under four Shared Socioeconomic Pathways (SSP) scenarios
- The diversity of strong ENSO-related ST response to different SSP scenarios is weaker than for moderate and weak ENSO-related ST responses
- The role of El Nino intensity on the diversity of ST anomalies is stronger in the sustainable SSP126 than for the business-as-usual SSP585

Supporting Information:

Supporting Information may be found in the online version of this article.

Correspondence to:

S.-W. Yeh and G. Wang,
swyeh@hanyang.ac.kr;
guojian.wang@csiro.au

Citation:

Yeh, S.-W., Wang, G., Cai, W., & Park, R. J. (2022). Diversity of ENSO-related surface temperature response in future projection in CMIP6 climate models: Climate change scenario versus ENSO intensity. *Geophysical Research Letters*, *49*, e2021GL096135. https://doi.org/10.1029/2021GL096135

Received 12 SEP 2021
Accepted 21 JAN 2022

Author Contributions:

Conceptualization: Sang-Wook Yeh, Guojian Wang
Formal analysis: Guojian Wang
Investigation: Sang-Wook Yeh, Guojian Wang
Methodology: Guojian Wang
Writing – original draft: Sang-Wook Yeh
Writing – review & editing: Guojian Wang, Wenju Cai, Rokjin J. Park

Diversity of ENSO-Related Surface Temperature Response in Future Projection in CMIP6 Climate Models: Climate Change Scenario Versus ENSO Intensity

Sang-Wook Yeh[1], Guojian Wang[2,3,4], Wenju Cai[2,3,4], and Rokjin J. Park[5]

[1]Department of Marine Sciences and Convergence Technology, Hanyang University, Ansan, South Korea, [2]Frontier Science Centre for Deep Ocean Multispheres and Earth System and Physical Oceanography Laboratory, Ocean University of China, Qingdao, China, [3]Qingdao National Laboratory for Marine Science and Technology, Qingdao, China, [4]Centre for Southern Hemisphere Oceans Research (CSHOR), CSIRO Oceans and Atmosphere, Hobart, Tas, Australia, [5]School of Earth and Environmental Sciences, Seoul National University, Seoul, South Korea

Abstract Few studies explore how the diversity of El Niño and Southern Oscillation (ENSO)-related atmospheric response is influenced by anthropogenic forcing and ENSO intensity. We examine the diversity of surface temperature (Ts) anomalies related to weak, moderate and strong ENSO events in North America (NA) for present and future climates forced under four Shared Socioeconomic Pathways (SSP) scenarios in CMIP6 climate models. When ENSO intensity is weaker, the NA Ts anomalies are more sensitive/variable to different SSP scenarios than moderate and strong ENSO. The NA Ts anomalies are more sensitive to the impacts of ENSO intensity under a sustainable climate change scenario, compared to the high SSP scenario. We discuss why the diversity of ENSO-related Ts response projections differs in the combination of ENSO intensity and climate change scenarios.

Plain Language Summary Both El Niño and Southern Oscillation (ENSO) amplitude and anthropogenic forcing scenario can exert a significant influence on the diversity of ENSO-related surface temperature (Ts) response in North America. Using a single CMIP6 model, the projected Ts response to strong ENSO events is less diverse from low to high radiative forcing than that to moderate and weak ENSO events, while the NA Ts anomalies are more sensitive to the impacts of ENSO intensity under a sustainable climate change scenario, compared to the high Shared Socioeconomic Pathways scenario. Therefore, the diversity of ENSO-related Ts response projections may differ in the combination of different ENSO intensity and climate change scenarios.

1. Introduction

The El Niño-Southern Oscillation (ENSO) severely impacts global weather and climate as well as regional socio-economic condition by causing extreme, devastating events such as heavy precipitation, droughts and heatwaves (Cai et al., 2014, 2015; 2017, 2018; McPhaden et al., 2006; Taschetto et al., 2020; Vincent et al., 2011; Wang et al., 2020). Improving the reliability of ENSO projections and understanding of the ENSO-related responses is important to the climate science community and the public.

ENSO influences global and regional temperature and precipitation variability via atmospheric teleconnection, which refers to concurrent or unsynchronized statistically significant ENSO-coherent fluctuations of an atmosphere field remote from the central-to-eastern equatorial Pacific directly or indirectly by ENSO-related sea surface temperature (SST) anomalies (Alexander et al., 2002; Yeh et al., 2018). The atmospheric teleconnection plays a key role in inducing the anomalous temperature and precipitation in the eastern Pacific-Atlantic sector's boreal winter, December–January–February (DJF), and significantly influences the socio-economic conditions in North America (NA) (Chen et al., 2018; Horel & Wallace, 1981; Michel et al., 2020; Zhou et al., 2014). However, there are considerable differences in strength and spatial pattern in the surface temperature (Ts) as well as precipitation anomalies in different El Niño and La Niña years in the globe including NA (Choidi & Harrison, 2013; Harrison & Larkin, 1998; Yu et al., 2012).

Furthermore, current Coupled Model Intercomparison Project (CMIP)-type climate models including Phase 3, 5, and 6 still have trouble in simulating the observed trend in SST across the tropical Pacific (Seager et al., 2019)

and there exists large uncertainties in how ENSO teleconnections would change from the present climate to future climate. In spite of such uncertainties (e.g., Beobide-Arsuaga et al., 2021; Fredriksen et al., 2020; Ma et al., 2012; Meehl & Teng, 2007; Sohn et al., 2018; Stevenson, 2012; Tedeschi & Collins, 2017), there is growing evidence showing that projected changes in ENSO amplitude affect ENSO atmospheric teleconnection projections (Taschetto et al., 2020). These lead to changes in ENSO-related Ts and precipitation response in NA. For example, different ENSO intensity can impose different impacts on NA in winter (e.g., Deser et al., 2017, 2018; Hoell et al., 2016; Jong et al., 2016). In addition, some studies argued that ENSO spatial pattern is one of the factors leading to the diversity in ENSO-related Ts in the Pacific and its rim (He et al., 2021; Weng et al., 2009). These results suggest that there are two main factors leading to the diversity in ENSO-related atmospheric anomalies, which are ENSO properties and anthropogenic forcings. For example, a recent study (Yang et al., 2021) using CMIP6 climate models found that in a warming climate, an El Niño-like eastern Pacific warming reduced NA monsoon rainfall as a result of the equatorward shift of the intertropical convergence zone.

Until now, however, few studies explored how the diversity of ENSO-related Ts is influenced by either ENSO intensity or climate change scenario, respectively, in the latest CMIP6 climate models. In addition to the understanding of future projection of Ts in NA, this analysis is also helpful to clarify the dominant factors influencing the predictability of ENSO-related Ts in a changing climate. In this work, we examine the diversity of ENSO-related Ts anomalies associated with weak, moderate and strong ENSO phenomena in NA with current climate (1950–1999) and future climate projections (2050–2099) using four Shared Socioeconomic Pathways (SSP) scenarios from a single climate model. The reason of why we focused on Ts in NA is because the CMIP-type climate models simulate better Ts than the precipitation, in addition, it is known that the response of ENSO forcing is distinct in NA via the atmospheric teleconnections (Cai et al., 2020; Yan et al., 2020). Therefore, the potential role of climate model biases in the diversity of ENSO-related atmospheric response could be suppressed by analyzing the Ts in NA.

2. Data and Methodology

2.1. Data

We mainly used a single realization of the CMIP6 Community Earth System Model version 2 Whole Atmosphere Community Climate Model (CESM2-WACCM) with a horizonal resolution of 288 × 192 longitude/latitude (Danabasoglu, 2019; Eyring et al., 2016) to explore the ENSO-related Ts anomalies over the NA. Data including SST and Ts forced under historical forcing to 2014 and four different Shared Socioeconomic Pathways to 2100, that is, SSP 1–2.6 (SSP126), 2–4.5 (SSP245), 3–7.0 (SSP370), and 5–8.5 (SSP585), are utilized. There is an inconsistency in the number of realizations of CESM2-WACCM under different emission scenarios, with only one realization under SSP126, 5 realizations under SSP245, 3 realizations under SSP370, and 5 realizations under SSP585 (https://pcmdi.llnl.gov/CMIP6/). For an equal weight, we only used the first realization of CESM2-WACCM in each scenario. This can also highlight differences due to external forcing along with internal variability across different emission scenarios in the same realization of CESM2-WACCM. It may be difficult to identify the role of internal variability on the ENSO-related Ts anomalies over the NA if we use different realizations in which the magnitude of internal variability is not the same.

CO_2 concentrations by 2100 range from 446, 603, 867, to 1135 ppm for the SSP126, SSP245, SSP370, and SSP585 emission scenarios respectively (Meinshausen et al., 2020). Although there are CMIP6 climate models from which all emission scenarios are available, most of them have had trouble to simulate the strengthening zonal SST gradient across the tropical Pacific in observations (Seager et al., 2019), which is critical to correctly project ENSO variability in future climate. CESM2-WACCM is one model that could follow observed trend with a statistical significance in recent decades (Figure S1 in Supporting Information S1) and it is one model that can simulate realistic ENSO characteristics, for example, nonlinear response of zonal winds associated with positive SST anomalies (Cai et al., 2020). In addition to CESM2-WACCM, we also analyzed six CMIP6 climate models including GFDL-ESM4, GISS-E2-1-G, MIROC6, MPI-ESM1-2-LR, MCM-UA-1-0, and FGOALS-g3.

We used data from 1950 to 1999 with historical forcing to represent the present-day climate and from 2050 to 2099 with four different emission scenarios to represent the projected future climate. We focused on the boreal winter season (DJF), when the ENSO intensity peaks and the associated atmospheric teleconnections can also

significantly influence Ts in NA (Horel & Wallace, 1981; Zhou et al., 2014). Unless stated otherwise, our results are for the boreal winter season (DJF) only.

2.2. ENSO Intensity

To gauge present-day ENSO intensity, we used the Niño3.4 index (5°N–5°S, 170°W–120°W). The Niño3.4 monthly index forced under historical forcing and all future emission scenarios is calculated first referenced to the monthly climatology over a common period from 1850 to 1899, and then quadratically detrended over each period. To enable the comparability across different emission scenario, the monthly detrended Niño3.4 index is then normalized by the standard deviation of Niño3.4 index over the common period from 1850 to 1899. Detrending the Niño3.4 index using a linear method did not change our results. We defined a weak El Niño event as when the Niño3.4 index is greater than 0.5 standard deviation (S.D.) and less than 1.0 S.D., a moderate El Niño event as when the Niño3.4 index is greater than 1.0 S.D., and less than 1.5 S.D.; and a strong El Niño event as when the Niño3.4 index is greater than 1.5 S.D. For example, a weak El Niño in 2050–2099 is defined as the Niño3.4 SST anomalies during 2050–2099 are between 0.5 and 1.0 S.D.. S. D is obtained from the Niño3.4 SST variance during 1850–1899. We defined weak, moderate, and strong La Niña events following the same criteria as the El Niño events, but with negative Niño3.4 thresholds. Figure S2 and S3 in Supporting Information S1 display the SST composites during weak, moderate, and strong El Niño and La Niña events for the four SSP scenario with a statistical significance. Table S1 in Supporting Information S1 provides how many events are used in each composite. To increase our confidence, we calculated observed ENSO-related Ts anomalies using SST from HadISSTs v1.1 with a horizonal resolution of 1 × 1 latitude/longitude (Rayner et al., 2003) and Ts from NCEP/NCAR reanalysis 1 (2.5 × 2.5 latitude/longitude grid; Kistler et al., 2001) for 1950–1999 and compared the results with our simulated patterns.

3. Results

3.1. Diversity of ENSO-Related Ts Response Due to ENSO Intensity in the Present Climate

The El Niño impact on Ts anomalies over NA is traditionally characterized as a north-south dipole pattern in the observation in which warmer-than-normal surface temperatures are found over the northern regions and colder-than-normal temperatures over the southeastern states (Figure 1a). La Niña generally leads to an opposite Ts response (Figure 1i). Similar patterns are observed in weak, moderate and strong El Niño (Figures 1b–1d) and La Niña (Figures 1j, 1k, and 1l) although there exist some discrepancies depending on ENSO intensity. This implies that ENSO intensity causes the diversity of ENSO-related Ts in NA during the present climate.

We examined whether CESM2-WACCM simulates accurate ENSO-related Ts spatial pattern anomalies in NA during the present climate. Figures 1e and 1m show the simulated composite Ts anomalies associated with all El Niño and La Niña events and the pattern correlations are 0.55 and 0.53, respectively, compared to the observations. CESM2-WACCM simulates features of El Niño/La Niña-related Ts response in NA during weak (Figures 1f and 1n), moderate (Figures 1g and 1o) and strong (Figures 1h and 1p) events in which there are some similarities and differences compared to the observations. El Niño-related Ts response diversity due to intensity is evident similar as the observation. While all types of El Niño-related Ts anomalies are characterized by a cooler-than-normal response in the southeastern NA (Figure 1e), there are large Ts response discrepancies outside this region (Figures 1f–1h). This indicates that El Niño events with different intensities can cause a large diversity of Ts anomalies in a climate model like the observation. As indicated by the pattern correlations, the typical El Niño-related Ts response characterized as a north-south dipole pattern (Figure 1e) is more evident during strong El Niño events than weak or moderate one (Figure 1h vs. Figures 1f and 1g). In contrast, weak, moderate, and strong La Niña-related Ts responses are spatially similar (Figures 1n–1p). All types of La Niña-related Ts anomalies are characterized by a warmer-than-normal southeastern NA and a cooler-than-normal northern NA. This implies that the diversity of La Niña-related Ts response due to intensity is weaker than for El Niño in the present climate.

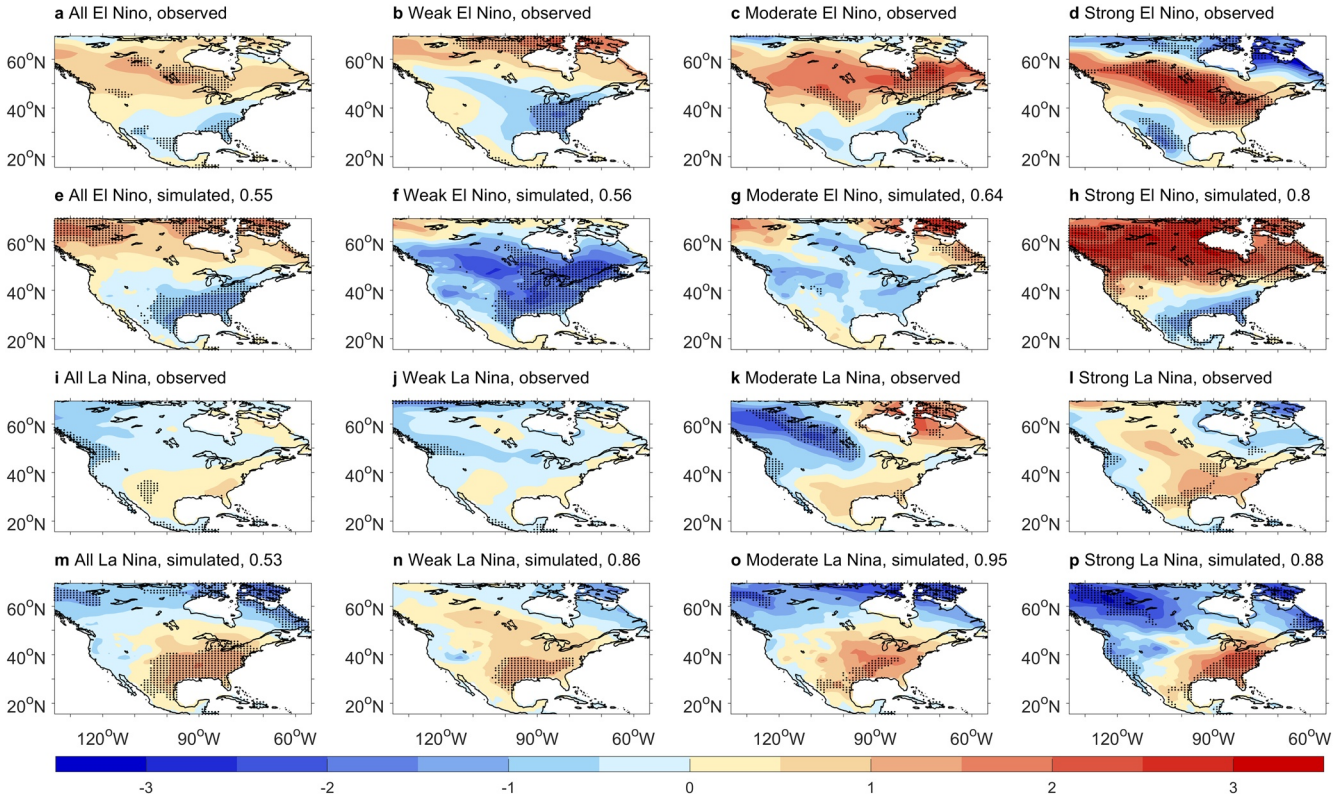

Figure 1. Observed and simulated El Niño and Southern Oscillation event surface temperature anomaly response over North America during 1950–1999. (a), (b), (c), and (d), Surface temperature anomaly composites (°C) during all El Niño, weak El Niño, moderate El Niño, strong El Niño events from observation data, respectively. (e), (f), (g), and (h), Surface temperature anomaly composites during all El Niño, weak El Niño, moderate El Niño, strong El Niño events from present-day climate simulations, respectively. The decimals in the titles of f to h are the pattern correlation coefficients between pattern shown in each panel and pattern shown in e, while decimal in the title of e indicates the pattern correlation between that and pattern shown in (a), (i), (j), (k), and (l), Surface temperature anomaly composites during all La Niña, weak La Niña, moderate La Niña, strong La Niña events from observation data, respectively. (m), (n), (o), and (p), Surface temperature anomaly composites during all La Niña, weak La Niña, moderate La Niña, strong La Niña events from present-day climate simulations, respectively. The decimals in the titles of n to p are the pattern correlation coefficients between pattern shown in each panel and pattern shown in m, while decimal in the title of m indicates the pattern correlation between that and pattern shown in (i) The dotted areas indicate where the composites are statistically different to zero above 90% confidence level based on a Student's t test.

3.2. Diversity of ENSO-Related Ts Response Due to ENSO Intensity and SSP Scenario in Future Climate

To explore the role of ENSO intensity and climate change scenario on ENSO-related Ts response in NA, we conduct a composite analysis using Ts anomalies during weak, moderate, and strong ENSO events during 2050–2099 for four different emission scenarios, that is, SSP126, SSP245, SSP370, and SSP585. Ts anomalies are calculated following the same method for the Niño3.4 index but without normalization. To quantify the diversity of ENSO-related Ts response, in addition, we calculate the pattern correlations between each ENSO-related Ts response in future climate and its corresponding composite simulated during the present climate (see decimals in Figure 2 and Figure 3). The pattern correlation in Figures 2 and 3 are calculated as the correlation between ENSO induced Ts anomalies over NA (225°E−310°E, 15°N–70°N) under SSP emission scenarios and that under historical forcing.

In weak El Niño events (Figures 2a–2g, and 2j), there is a high diversity of El Niño-related Ts response under SSP126, SSP245, SSP370, and SSP585 scenarios, which is also confirmed in the pattern correlations. For example, the Ts anomalies pattern (warm northwest-cold southeast) is very different under SSP370 compared to the other SSP scenarios and the present climate (Figure 2g vs. Figures 2a–2j). This is also confirmed from the Pacific-North America (PNA) teleconnections obtained from the 500 hPa geopotential composite during El Niño events (Figure S4 in Supporting Information S1), indicating that a dipole-like geopotential height at 500 hPa disappears over NA under SSP370 (Figure 2g and S4g in Supporting Information S1). It is also found that the diversity of tropical Pacific precipitation pattern associated with a weak El Niño from SSP126 to SSP585 is the

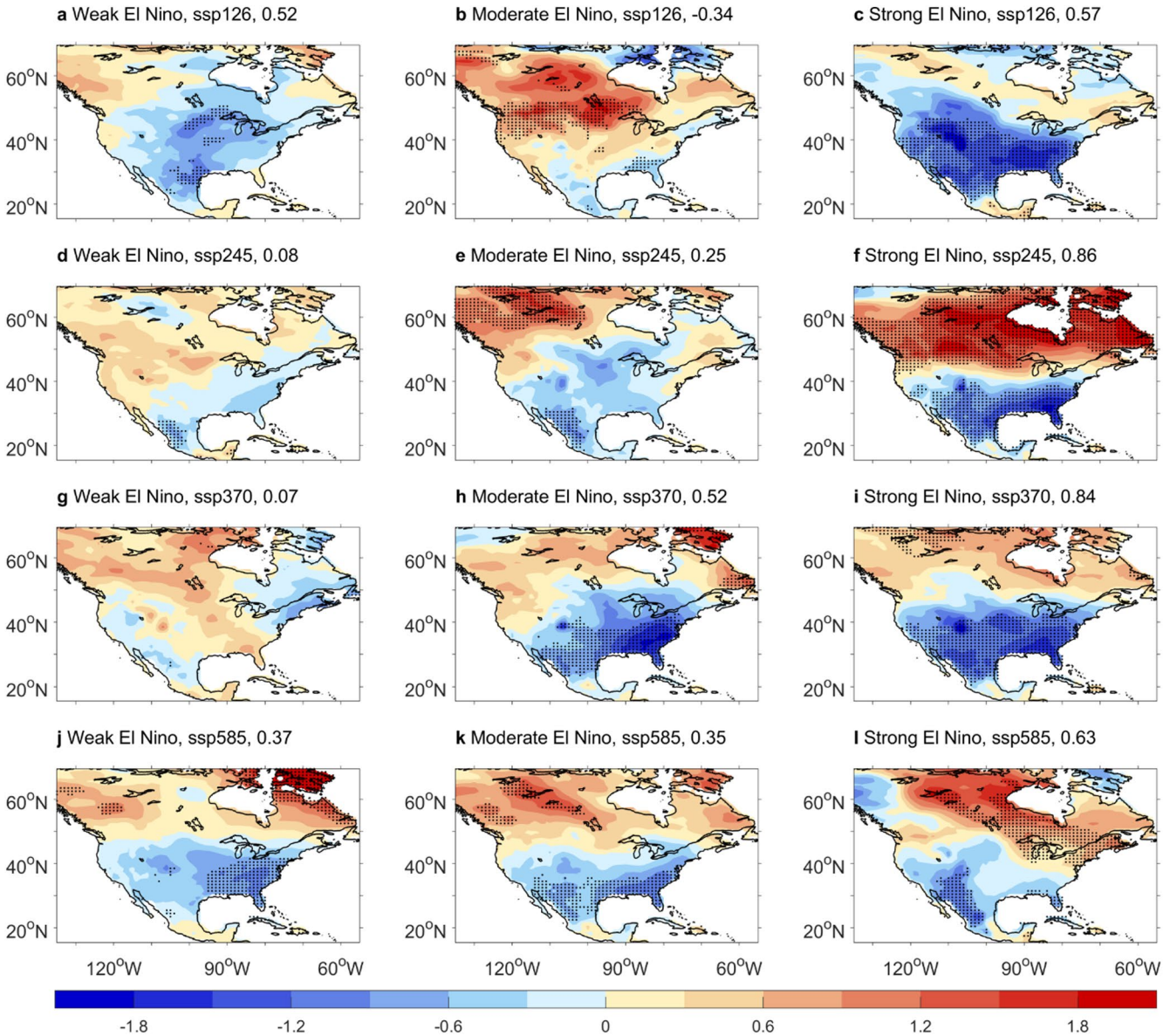

Figure 2. Projected North American El Niño surface temperature anomaly responses to future emission scenarios. Surface temperature anomaly composites (°C) during weak, moderate, and strong El Niño events for the SSP126 scenario (a), (b), and (c), SSP245 scenario (d), (e), and (f), SSP370 scenario (g), (h), and (i), and SSP585 scenario (j), (k), and (l). The dotted areas indicate where the composites are statistically different to zero above 90% confidence level based on a Student's *t* test. The decimals in the titles are the pattern correlation coefficients between each panel and its corresponding composite simulated during the present climate, that is, (a), (d), (g), (j) versus Figures 1b, 1f; 1e, 1h, and 1k versus Figures 1g, 1c, 1f, 1i, and 1l versus Figure 1h.

largest compared with those in moderate and strong El Niño (Figure S5 in Supporting Information S1), which is also consistent with the diversity of PNA teleconnections (Figure S4 in Supporting Information S1). This weak El Niño-related Ts response diversity could be due to the nonlinear interactions with different climate change scenarios, which makes El Niño-related Ts patterns be more various when El Niño is weak. We infer that the anthropogenic forcing from SSP126 to SSP585 scenario acts to enhance the diversity of a weak El Niño-related Ts response with the changes in mean SST in the tropics, which will be discussed later. However, we cannot exclude another possibility that the weaker El Niño events are easier outplayed by internal variability. As such, the diversity of Ts response to weak El Niño events might not be due to any nonlinear interaction between El Niño and climate change, but rather simply due to internal variability (Deser et al., 2017, 2018).

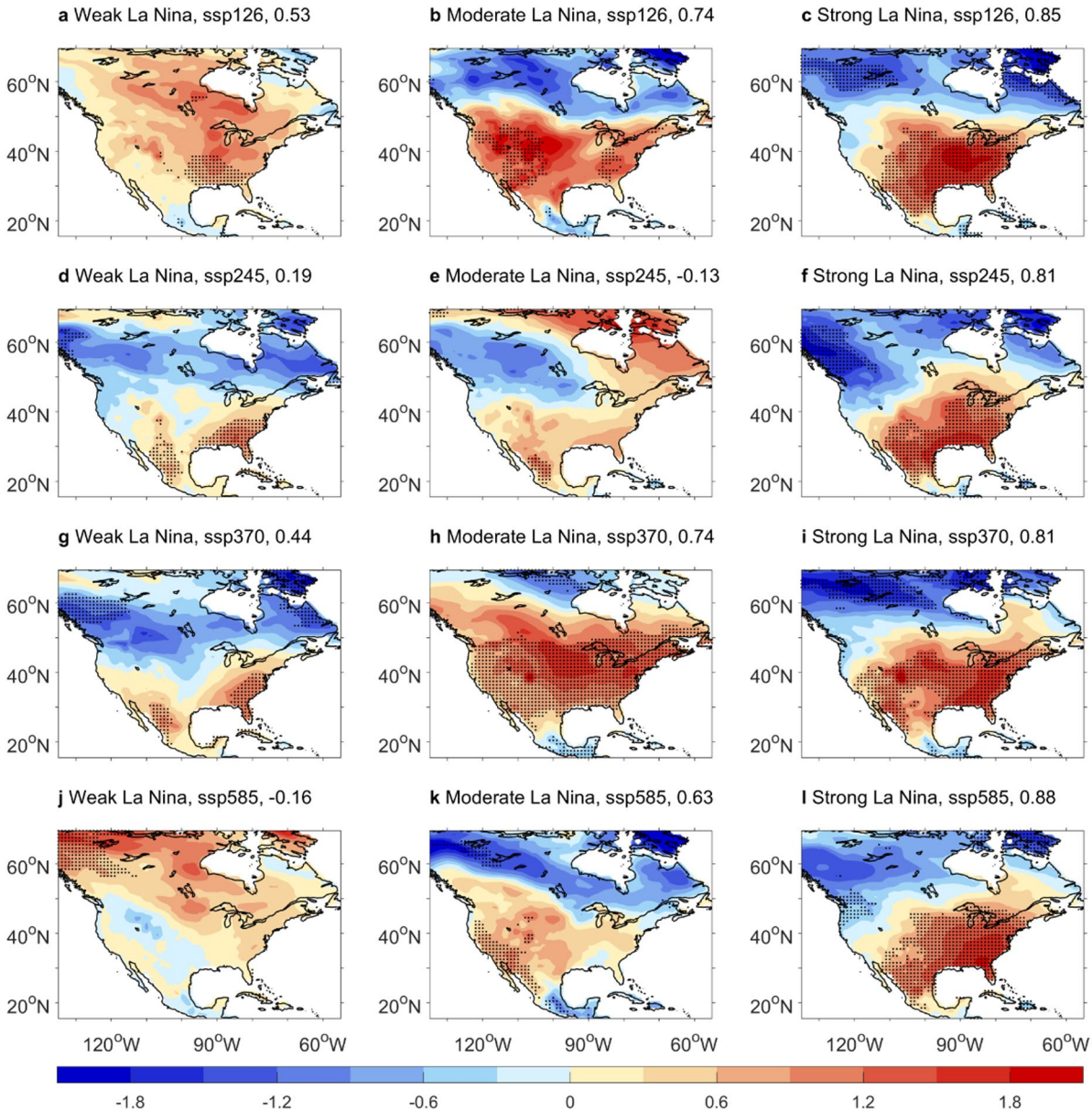

Figure 3. Projected North American La Niña surface temperature anomaly responses to future emission scenarios. Surface temperature anomaly composites (°C) during weak, moderate, and strong La Niña events under the SSP126 scenario (a), (b), and (c), SSP245 scenario (d), (e), and (f), SSP370 scenario (g), (h), and (i), and SSP585 scenario (j), (k), and (l). The dotted areas indicate where the composites are statistically different to zero above 90% confidence level based on a Student's *t* test. The decimals in the titles are the pattern correlation coefficients between each panel and its corresponding composite simulated during historical period, that is, (a), (d), (g), (j) versus Figures 1b, 1e, 1h, 1n, 1and 1k versus Figures 1c, 1f, 1i, 1o, and 1l versus Figure 1p.

In the three higher SSP scenarios of SSP245, SSP370, and SSP585, a north-south dipole pattern of strong (Figures 2f, 2i and 2l) and moderate (Figures 2e–2k) El Niño-related Ts anomalies dominates which is consistent with high pattern correlations, while such pattern is less evident in weak El Niño-related Ts (Figures 2d–2j). Indeed, the pattern correlations, which are obtained by comparing with strong El Niño-related Ts during the present climate, are larger in higher SSP scenarios (Figures 2f, 2i, and 2l) than lower SSP scenario (Figure 2c). This highlights that climate change scenario plays a part in altering Ts patterns associated with El Niño intensity.

We also examine the intensity impacts on El Niño-related Ts responses using the same SSP scenario and found a diversity of weak, moderate and strong El Niño-related Ts responses under the same emission scenarios (Figures 2a–2l). This indicates that El Niño intensity causes Ts response diversity via PNA atmospheric

teleconnections despite under the same emission scenario. In the SSP585 scenario (Figures 2j–2l), however, a north-south Ts anomaly dipole pattern is evident in all weak, moderate and strong El Niño, which is in contrast to that in the SSP126 scenario (Figures 2a–2c). The diversity of pattern correlations is the weakest (largest) in SSP585 (SSP126) scenario. These results imply that while El Niño intensity may not impact the diversity of response in the business-as-usual scenario SSP585, it can apply strong influence in sustainability scenario SSP126.

Figure 3 is the same as in Figure 2 except for weak, moderate and strong La Niña-related Ts response. Similar to El Niño-related Ts response, there is a diversity of weak La Niña-related Ts spatial pattern and intensity under the SSP126, SSP245, SSP370, and SSP585 scenarios (Figures 3a–3g, and 3j). The warmer-than-normal Ts anomalies related to a weak La Niña is simulated in most NA regions under the SSP126 scenario (Figure 3a), which is different to that under the SSP245, SSP470, and SSP585 scenarios (Figures 3d–3j). When compared to moderate (Figures 3b–3h, and 3k) and strong (Figures 3c–3i, and 3l) events, the Ts pattern associated with La Niña is the most diverse during weak La Niña events based on their pattern correlations. In other words, weak La Niña-related Ts responses are largely modified by anthropogenic forcing from SSP126 to SSP585 scenario. In addition, the pattern correlations in strong La Niña-related Ts responses are larger than 0.8 in all scenarios (Figures 3c–3i and 3l) and their diversity is small, implying that anthropogenic forcings from SSP126 to SSP585 scenarios do not significantly modify the response of strong La Niña-related Ts anomalies. This may imply that the strongest La Niña is not outplayed by anthropogenic forcing as weak La Niña. This notion is also confirmed by the PNA teleconnections based on a composite analysis using 500 hPa geopotential anomalies during weak, moderate, and strong La Niña events for four different emission scenarios (Figure S6 in Supporting Information S1).

We also examine intensity impacts on the diversity of La Niña-related Ts response using the same SSP scenario. We find a diversity of weak, moderate and strong La Niña-related Ts responses under the SSP126 (Figures 3a–3c), SSP245 (Figures 3d–3f), SSP370 (Figures 3g–3i) and SSP585 (Figures 3j–3l) scenarios based on their pattern correlations, implying that La Niña intensity plays a role in the diversity of Ts response under the same SSP scenario. High pattern correlations are found in SSP126 and SSP370 compared to SSP245 and SSP585. In particular, the diversity of pattern correlations is small in SSP126 scenario (Figures 3a–3c) compared to other scenarios, which is in contrast to that in El Niño-related Ts response. These asymmetric responses/changes between El Niño and La Niña in different scenarios could be explained by the change in the relationship between the total SST and the deep convective activities over the central-to-eastern tropical Pacific, which will be discussed later.

Figure 4 summarizes the relationship between ENSO intensity and North American Ts spatial pattern anomalies for SSP126, SSP245, SSP370, and SSP585 scenarios. There is a significant feature that the diversity of ENSO-related Ts response is reduced (high pattern correlation) during strong ENSO event (Figures 4a and 4b, star). In other words, the diversity of strong ENSO-related Ts response from SSP126 to SSP585 scenarios is weaker than for weak ENSO-related Ts responses. In addition, the role of intensity on the diversity of El Niño-related Ts response tends to be weaker for the business-as-usual SSP585 scenario than that for the sustainability SSP126 scenario (Figures 4c and 4d). To obtain the robustness of the results obtained from a single realization of CESM2-WACM, we further analyzed six CMIP6 climate models (GFDL-ESM4, GISS-E2-1-G, MIROC6, MPI-ESM1-2-LR, MCM-UA-1-0, and FGOALS-g3) for SSP126, SSP245, SSP370, and SSP585 scenarios (Figures S7–S12 in Supporting Information S1). Generally, there is a strong model consensus in the relationship between ENSO intensity and the diversity of Ts response in NA under four SSP scenarios. In addition, the diversity of El Niño-related Ts response tends to be weaker for the higher SSP585 scenario than that for the lower SSP126 scenario. This notion could be explained as follows. Under the SSP585 scenario, the tropical precipitation anomalies extend further eastward during El Niño events regardless of El Niño intensity (Figures S5j–S5l in Supporting Information S1). This is because the climatological SST is much warmer under the SSP585. It is therefore much easier for deep convection to grow over the eastern tropical Pacific, compared to the present climate or the lower SSP126 scenario. Since the linear relationship between total SST and deep convective activities only sustains below certain SST threshold (~29.5°C, e.g., Waliser et al., 1993), the intensity of SST anomalies would play a less important role in inducing anomalous deep convective activities and therefore teleconnections in the much warming climate.

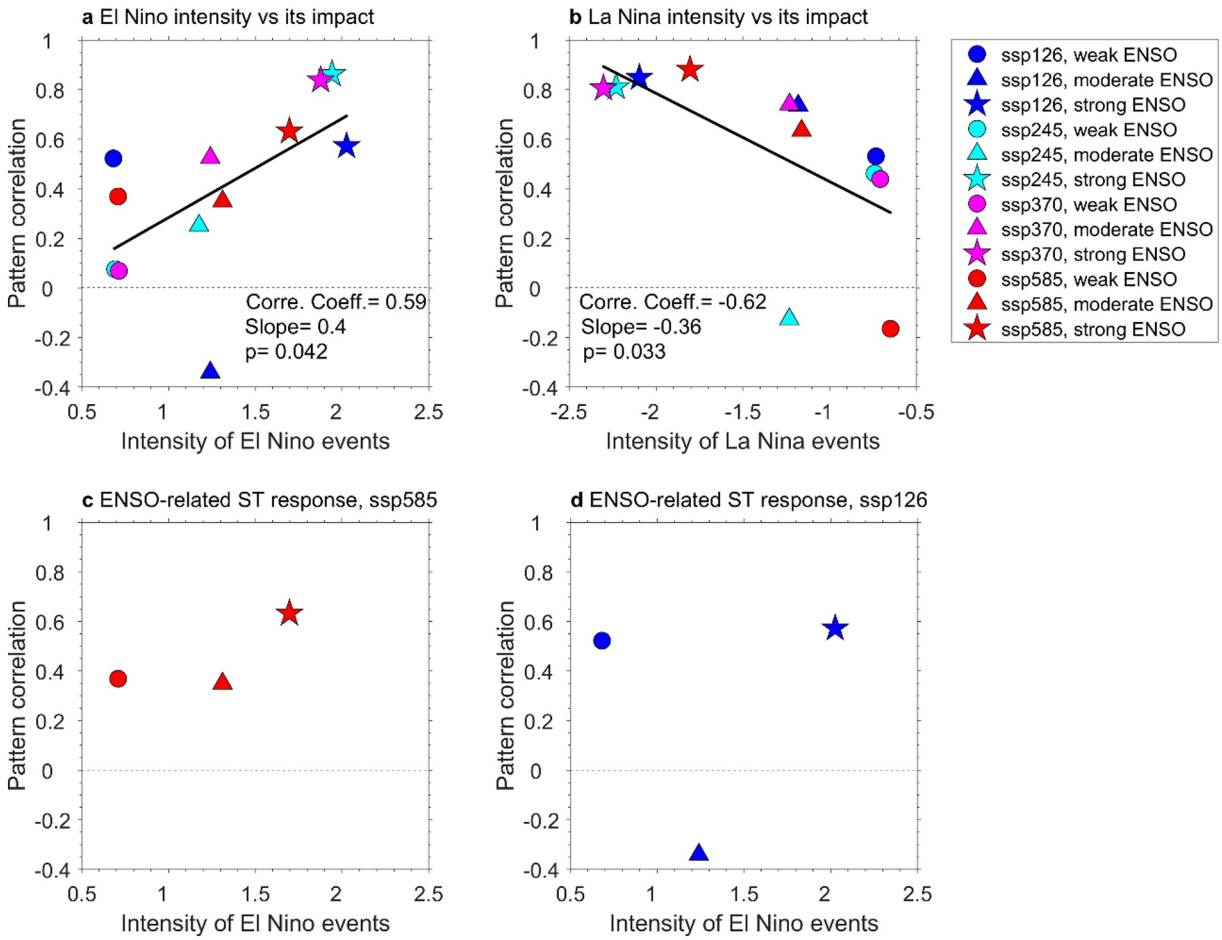

Figure 4. Relationship between El Niño and Southern Oscillation (ENSO) intensity and North American Ts spatial pattern anomalies for SSP126, SSP245, SSP370, and SSP585 scenarios. ENSO-related spatial patterns for NA Ts anomalies are represented as pattern correlations between projected ENSO-related Ts patterns and their corresponding Ts patterns simulated using present-day climate data (Figures 1e–1j). (a) and (b) spread during El Niño and La Niña events, respectively. (c) and (d) spread for all El Niño events forced under SSP585 and SSP126 scenarios, respectively.

4. Summary

While the present study did not focus on the physical mechanisms of how ENSO teleconnections and their remote impacts change under different ENSO intensity and SSP scenario, we conducted a quantitative analysis to examine the roles of climate change scenario and ENSO intensity on the diversity of ENSO-related NA Ts responses. Both climate change scenarios and ENSO intensity caused a diversity of ENSO-related Ts responses. However, we also found that the response diversity due to climate change scenario differs depending on whether ENSO intensity is weak or strong. Diversity also arises from ENSO intensity, which differs from SSP126 to SSP585 scenarios. Different time windows, for example, 1900–1999 versus 2000–2099, generate similar results (figure not shown). Therefore, our results are less likely to be influenced by a sampling issue or decadal ENSO variability modulation. The following are our main findings.

1. The diversity of El Niño-related Ts response is smaller in the highest SSP scenario than that the lowest SSP scenario
2. The diversity of strong El Niño/La Niña-related Ts response from SSP126 to SSP585 scenarios is weaker than for weak El Niño/La Niña-related Ts responses. Such phenomena are more evident in La Niña-related Ts response than El Niño
3. The role of El Niño intensity on El Niño-related Ts response diversity tends to be weaker for the business-as-usual SSP585 scenario than the sustainability SSP126 scenario

These findings are mainly based on a single realization of CESM2-WACCM and the key message is also conveyed by additional six CMIP6 climate models. The mechanism behind that the ENSO induced Ts is less variable in NA during stronger ENSO events (Figures 4a and 4b) could be built on the well-recognized PNA pattern due to ENSO induced Rossby wave train (see also Figures S4 and S6 in Supporting Information S1), that is, stronger ENSO leading to stronger ENSO teleconnection. The notion that the spread during lower emission scenario is larger than that during higher emission scenario (Figures 4c and 4d) is likely due to the fact that the response of weak El Niño events are easier overwhelmed by internal variability in lower emission scenario than that in higher emission scenario forced under which an El Niño-like warming pattern along tropical Pacific Ocean is projected (Cai et al., 2015). Despite this, the respective roles that internal variability and external forcing play in modulating ENSO teleconnections are still unclear. This requires a designated model simulation with large ensemble realizations, which will be explored further in another study.

Conflict of Interest

The authors declare no conflicts of interest relevant to this study.

Data Availability Statement

NCEP/NCAR reanalysis 1 can be downloaded from https://psl.noaa.gov/data/gridded/data.ncep.reanalysis.html; HadISST from https://www.metoffice.gov.uk/hadobs/hadisst/data/download.html; CESM2-WACCM from https://pcmdi.llnl.gov/CMIP6/.

Acknowledgments
SWY was supported by the National Research Foundation of Korea (NRF) grant (NRF-2018R1A5A1024958). This research was also supported by the Research Program for the carbon cycle between oceans, land, and atmosphere of the NRF funded by the Ministry of Science and ICT (2021M3I6A1086794). GW and WC is supported by the Centre for Southern Hemisphere Oceans Research, a joint research center between QNLM and CSIRO, and also by the Australian Government under the National Environmental Science Program.

References

Alexander, M. A., Blade, I., Newman, M., Lanzante, J. R., Lau, N. C., & Scott, J. D. (2002). The atmospheric bridge: The influence of ENSO teleconnections on air–sea interaction over the global oceans. *Journal of Climate*, *15*, 2205–2231.

Beobide-Arsuaga, G., Bayr, T., & Reintges, A. (2021). Uncertainty of ENSO-amplitude projections in CMIP5 and CMIP6 models. *Climate Dynamics*, *56*. https://doi.org/10.1007/s00382-021-05673-4

Cai, W., Borlace, S., Lengaigne, M., van Rensch, P., Collins, M., Vecchi, G., et al. (2014). Increasing frequency of extreme El Niño events due to greenhouse warming. *Nature Climate Change*, *4*, 111–116. https://doi.org/10.1038/nclimate2100

Cai, W., McPhaden, M., Grimm, A. M., Rodrigues, R. R., Taschetto, A. S., Garreaud, R. D., et al. (2020). Climate impacts of the El Niño-southern oscillation on South America. *Nature Reviews Earth & Environment*, *1*, 215–231.

Cai, W., Santoso, A., Wang, G., Yeh, S.-W., An, S.-I., Cobb, K. M., et al. (2015). ENSO and greenhouse warming. *Nature Climate Change*, *5*, 132–137. https://doi.org/10.1038/nclimate2743

Cai, W., Wang, G., Dewitte, B., Wu, L., Santoso, A., Takahashi, K., et al. (2018). Increased variability of eastern Pacific El Niño under greenhouse warming. *Nature*, *564*, 201–206.

Cai, W., Wang, G., Santoso, A., Lin, X., & Wu, L. (2017). Definition of extreme El Niño and its impact on projected increase in extreme El Niño frequency. *Geophysical Research Letters*, *44*, 11184–11190.

Chen, Z., Gan, B., Wu, L., & Jia, F. (2018). Pacific-North American teleconnection and North Pacific oscillation: Historical simulation and future projection in CMIP5 models. *Climate Dynamics*, *50*, 4379–4403.

Choidi, A. M., & Harrison, D. E. (2013). El Niño impacts on Seasonal U.S. Atmospheric circulation, temperature, and precipitation anomalies: The OLR-event perspective. *Journal of Climate*, *26*, 822–837.

Danabasoglu, G. (2019). *NCAR CESM2-WACCM model output prepared for CMIP6 CMIP. Version YYYYMMDD*. Earth System Grid Federation. https://doi.org/10.22033/ESGF/CMIP6.10024

Deser, C., Simpson, I. R., McKinnon, K. A., & Phillips, A. S. (2017). The Northern Hemisphere extratropical atmospheric circulation response to ENSO: How well do we know it and how do we evaluate models accordingly? *Journal of Climate*, *30*, 5059–5082.

Deser, C., Simpson, I. R., Phillips, A. S., & McKinnon, K. A. (2018). How well do we know ENSO's climate impacts over North America, and how do we evaluate models accordingly? *Journal of Climate*, *31*, 4991–5014.

Eyring, V., Bony, S., Meehl, G. A., Senior, C. A., Stevens, B., Stouffer, R. J., & Taylor, K. E. (2016). Overview of the coupled model Intercomparison project phase 6 (CMIP6) experimental design and organization. *Geoscientific Model Development*, *9*(5), 1937–1958. https://doi.org/10.5194/gmd-9-1937-2016

Fredriksen, H.-B., Berner, J., Subramanian, A. C., & Capotondi, A. (2020). How does El Niño–Southern Oscillation change under global warming—a first look at CMIP6. *Geophysical Research Letters*, *47*, e2020GL090640. https://doi.org/10.1029/2020GL090640

Harrison, D. E., & Larkin, N. K. (1998). Seasonal U.S. temperature and precipitation anomalies associated with El Niño: Historical results and comparison with 1997–1998. *Geophysical Research Letters*, *25*, 3959–3962. 10.1029/1998GL900061

He, L., Hao, X., & Han, T. (2021). The asymmetric impacts of ENSO Modoki on boreal winter climate over the Pacific and its rim. *Climate Dynamics*, *56*, 29–44.

Hoell, A., Hoerling, M., Eischeid, J., Wolter, K., Dole, R., Perlwitz, J., et al. (2016). Does El Niño intensity matter for California precipitation? *Geophysical Research Letters*, *43*, 819–825. 10.1002/2015GL067102

Horel, J. D., & Wallace, J. M. (1981). Planetary-scale atmospheric phenomena associated with the Southern Oscillation. *Monthly Weather Review*, *109*, 813–829.

Jong, B.-T., Ting, M., & Seager, R. (2016). El Niño's impact on California precipitation: Seasonality, regionality, and El Niño intensity. *Environmental Research Letters*, *11*, 054021. https://doi.org/10.1088/1748-9326/11/5/054021

Kistler, R., Kalnay, E., Collins, W., Saha, S., White, G., Woollen, J., et al. (2001). The NCEP-NCAR 50-year reanalysis: Monthly means CDROM and documentation. *Bulletin of the American Meteorological Society*, *82*(2), 247–267.

Ma, J., Xie, S.-P., & Kosaka, Y. (2012). Mechanisms for tropical tropospheric circulation change in response to Global warming. *Journal of Climate*, *25*, 2979–2994.

McPhaden, M. J., Zebiak, S. E., & Glantz, M. H. (2006). ENSO as an integrating concept in Earth science. *Science*, *314*, 1740–1745.

Meehl, G. A., & Teng, H. (2007). Multi-model changes in El Niño teleconnections over North America in a future warmer climate. *Climate Dynamics*, *29*, 779–790.

Meinshausen, M., Nicholls, Z. R. J., Lewis, J., & Gidden, M. (2020). The shared socio-economic pathway (SSP) greenhouse gas concentrations and their extensions to 2500. *Geoscientific Model Development*, *13*, 3571–3605.

Michel, C., Li, C., Simpson, I. R., Bethke, I., King, M. P., & Sobolowski, S. (2020). The change in the ENSO teleconnection under a low Global warming Scenario and the uncertainty due to internal variability. *Journal of Climate*, *33*(11), 4871–4889.

Rayner, N. A., Parker, D. E., Horton, E. B., Folland, C. K., Alexander, L. V., Rowell, D. P., et al. (2003). Global analyses of sea surface temperature, sea ice, and night marine air temperature since the late nineteenth century. *Journal of Geophysical Research*, *108*, 4407. https://doi.org/10.1029/2002JD002670

Seager, R., Cane, M., Henderson, N., Lee, D. -E., Abernathey, R., & Zhang, H. (2019). Strengthening tropical Pacific zonal sea surface temperature gradient consistent with rising greenhouse gases. *Nature Climate Change*, *9*, 517–522.

Sohn, B.-J., Yeh, S.-W., Lee, A., & Lau, W. K. M. (2018). Regulation of atmospheric circulation controlling the tropical Pacific precipitation change in response to CO_2 increases. *Nature Communications*, *10*(1), 1–8.

Stevenson, S. L. (2012). Significant changes to ENSO strength and impacts in the twenty-first century: Results from CMIP5. *Geophysical Research Letters*, *39*, L17703. 10.1029/2012GL052759

Taschetto, A. S., Ummenhofer, C. C., Stuecker, M. F., Dommenget, D., Ashok, K., Rodrigues, R. R., & Yeh, S.-W. (2020). El Niño–southern oscillation atmospheric teleconnections. In M. J. McPhaden, A. Santoso, & W. Cai (Eds.), *El Niño southern oscillation in a changing climate*. *AGU Monograph*. https://doi.org/10.1002/9781119548164.ch14

Tedeschi, R. G., & Collins, M. (2017). The influence of ENSO on South American precipitation: Simulation and projection in CMIP5 models. *International Journal of Climatology*, *37*, 3319–3339.

Vincent, E. M., Lengaigne, M., Menkes, C. E., Jourdain, N. C., Marchesiello, P., & Madec, G. (2011). Interannual variability of the South Pacific convergence zone and implications for tropical cyclone genesis. *Climate Dynamics*, *36*, 1881–1896.

Waliser, D. E., Graham, N. E., & Gautier, C. (1993). Comparison of the highly reflective cloud and outgoing longwave radiation datasets for use in estimating tropical deep convection. *Journal of Climate*, *6*, 331–353.

Wang, G., Cai, W., & Santoso, A. (2020). Stronger increase in the frequency of extreme convective than extreme warm El Niño events under greenhouse warming. *Journal of Climate*, *33*, 675–690.

Weng, H., Behera, S. K., & Yamagata, T. (2009). Anomalous winter climate conditions in the Pacific rim during recent El Niño modoki and El Niño events. *Climate Dynamics*, *32*, 663–674.

Yan, Z., Wu, B., Li, T., Collins, M., Clark, R., Zhou, T., et al. (2020). Eastward Shift and extension of ENSO-induced tropical precipitation anomalies under Global warming. *Science Advances*, *6*, eaax4177.

Yang, Y.-M., Park, J.-H., An, S.-I., Wang, B., & Luo, X. (2021). Mean seat surface temperature changes influence ENSO-related precipitation changes in the mid-latitudes. *Nature Communications*, *12*, 1495.

Yeh, S.-W., Cai, W., Min, S.-K., McPhaden, M. J., Dommenget, D., Dewitte, B., et al. (2018). ENSO atmospheric teleconnections and their response to Greenhouse Gas forcing. *Reviews of Geophysics*, *56*, 185–206. https://doi.org/10.1002/2017RG000568

Yu, J.-Y., Zou, Y., Kim, S. T., & Lee, T. (2012). The changing impact of El Niño on US winter temperatures. *Geophysical Research Letters*, *39*, L15702. https://doi.org/10.1029/2012GL052483

Zhou, Z.-Q., Xie, S.-P., Zheng, X.-T., Liu, Q., & Wang, H. (2014). Global warming-induced changes in El Niño teleconnections over the north Pacific and North America. *Journal of Climate*, *27*, 9050–9064.